THE JOURNAL OF PHYSICAL CHEMISTRY C

ARTICLE

pubs.acs.org/JPCC

Mechanistic Aspect of Surface Modification on Glass Substrates Assisted by Single Shot Pulsed Laser-Induced Fragmentation of Gold Nanoparticles

Shuichi Hashimoto,*[,†] Takayuki Uwada,[‡] Masahide Hagiri,[†] and Ryowya Shiraishi[†]

[†]Department of Ecosystem Engineering, The University of Tokushima, Tokushima 770-8506, Japan

[‡]Department of Applied Chemistry and Institute of Molecular Science, National Chiao Tung University, Hsinchu 30010, Taiwan

Supporting Information

ABSTRACT: This paper describes the mechanistic investigation on the photomodification of a borosilicate glass substrate assembled with 47 ± 8 nm gold nanoparticles and exposed to a single shot of 532 nm nanosecond pulsed-laser light. The laser fluences ranging from 180 to 430 mJ cm^{-2} pulse^{-1}, the values of which are 2 orders of magnitude lower than the breakdown threshold of quartz of 15−20 J cm^{-2} pulse^{-1} were used. Upon photomodification, the craters of ∼20 nm diameter and ∼10 nm depth were formed on the glass surface simultaneously with the laser-induced splitting of Au nanoparticles to generate smaller particles of 15 nm diameter. The number density of the craters increased depending on the laser fluence with a sharp rise, the onset of which occurred at ∼160−170 mJ cm^{-2} pulse^{-1}, and reached a value of twice the number density of original Au particles (150 ± 10 particles μm^{-2}) with a weak tendency to level off at high fluences. The onset of the crater formation coincides with splitting of gold nanoparticles due to the temperature rise above the boiling point of gold resulting from the absorption of the laser energy. Thus, the explosive evaporation of gold nanoparticles is postulated to play a crucial role for the modification observed here. This assumption gained a solid support from the estimation of laser fluence-dependent thermoacoustic pressures due to the sudden evaporation of gold. This finding may represent a new application of the laser ablation/fragmentation of nanoparticles to material processing.

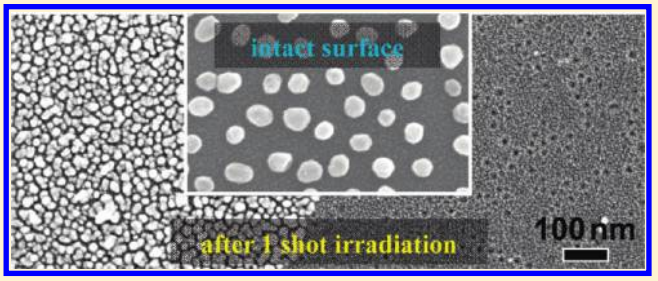

INTRODUCTION

Optical properties of noble metal nanopaticles (NPs) have attracted considerable attention because they exhibit extremely high absorption and scattering cross sections compared with any other inorganic and organic counterparts due to surface plasmon resonance.[1] Besides, NPs bears fascinating properties represented by the plasmonic enhancement[2] of an incident electromagnetic field which finds applications in ultratrace analyses utilizing SERS (surface-enhanced Raman scattering)[3,4] and plasmon-assisted photochemical reactions.[5,6] Furthermore, photothermal and photomechanical effects under short pulsed-laser excitation have drawn increasing attention in recent years.[7−9] In this regard, the laser energy absorbed by the particles can contribute to drastic changes in the strong absorber and surrounding medium. For instance, a sudden temperature rise can result in lattice expansion, melting, and vaporization of the particles themselves. Moreover, heating and vapor formation around the particles can take place simultaneously with pressure signals exhibited by acoustic waves and shockfronts. The laser-induced heat, bubbles and pressures have potential use in cancer therapy as a part of applications to nanomedicine. Furthermore, potential application of nanoparicles to a nanoscale material processing has been demonstrated.

Ko and co-workers reported the fabrication of nanometer-sized craters on a polyimide film self-assembled with Au NPs when exposed to a 532 nm nanosecond laser light through an objective lens (3−5 ns pulse width, 30−300 mJ cm^{-2} fluence).[10] Tsuboi and co-workers observed the nanohole formation on a Au NP−polymer hybrid film deposited on glass substrates and irradiated by a single 532 nm nanosecond pulsed laser shot.[11] These two studies ascribed the origin of nanoholes to the melting of the substrates due to heat transfer from the NPs. The heat mode of nanofabrication represents the material modification due to damages caused by melting and explosive evaporation of Au atoms and clusters generated through the rapid overheating of strongly absorbing NPs during a short laser pulse when the influence of heat diffusion is minimal. In the meantime, Obara and co-workers observed the formation of nanoholes on the surface of a silicon substrate deposited with Au nanospheres by irradiating a single femtosecond laser pulse having an intensity of less than the ablation threshold of silicon.[12−14] These reports attributed to the plasmonic enhancement of the incident electric field at the boundary of the NP and the substrate. Other groups

Special Issue: Laser Ablation and Nanoparticle Generation in Liquids

Received: July 22, 2010
Revised: November 1, 2010
Published: November 17, 2010

reported a similar finding to Obara's group.[15,16] Thus, besides the heat mode of enhanced material fabrication, a photon mode process is postulated to occur in which the electric field enhancement due to the excitation of the surface plasmon band of NPs can cause a multiphoton absorption leading to the ablation and modification of the material surface.

Although the laser technique is powerful and versatile in 3D microfabrication, a major drawback is its low throughput, in particular, in the femtosecond laser processing.[17,18] In this regard, investigations aiming at utilizing NPs and nanostructures to the laser material structuring are equally important for expanding the capability of nanomaterial-based technology to an unexplored field of nanofabrication as well as for developing the energy saving way of laser fabrication. Despite the nanohole fabrication on silicon and polymer surfaces has been reported upon the laser excitation of Au NPs as mentioned above, such attempts were rarely made on glass substrate. This is because the laser processing of the glass substrate by the application of NP-based approach is a more challenging task than the fabrication on the silicon substrate where a larger plasmonic enhancement is predicted due to its greater dielectric functions or the polymer surface with appreciably lower melting temperatures. In recent study, we have observed the laser photomodification, i.e., the formation of nanoscale craters at scattered places on a borosilicate glass surface assembled with Au NPs by exposure to multishots (10−36 000 shots) of 532 nm nanosecond pulsed laser beams with fluences less than 500 mJ cm^{-2} $pulse^{-1}$, well below the breakdown threshold of 25−40 J cm^{-2} $pulse^{-1}$.[19] The average diameter of the craters was ca. 10 nm at initial stages but repeated irradiations granted the size expansion of the craters to a hundred nanometer scale. Our observation of the craters is distinct from the previous observation of nanoholes on silicon substrate, where a single laser shot allowed the fabrication of a pit underneath a given Au NP, sugesting the plasmonic enhancement of the electromagnetic field.[12−16] We ascribed the mechanism of the crater formation primarily to the heat mode process but details were still not clear. Interestingly, the laser-modified area acquired an increased etching susceptibility to aqueous hydrofluoric acid and the selective etching of the irradiated area was achieved. The result strongly suggests the feasibility of Au NP-based laser structuring on the glass substrates. Although we observed the modification of the glass surface accompanied by the splitting of Au NPs by a number of laser shots, the process induced by the laser irradiation seems to be complicated because of the inhomogeneous size changes of the Au NPs. Therefore, the single laser shot experiment is prerequisite in order to attain deeper understanding of the mechanism. Here, we report the observation of the single-shot laser photomodification of glass surfaces along with the mechanistic investigation of the surface damage by calculating vapor pressures caused by the sudden evaporation of Au NPs.

EXPERIMENTAL SECTION

On average 40−50 nm diameter Au particles were prepared by citrate reduction in aqueous solution according to the literature.[20] The stock solution was made by dissolving 1 g of $HAuCl_4 \cdot 4H_2O$ (Wako Chemical, 99.9%) in 10 mL of doubly distilled water. A 100 mL aliquot of 0.1% $HAuCl_4$ aqueous solution prepared by diluting the stock solution 1000 times was heated and 1.1 mL of 1% trisodium citrate (Wako Chemical) aqueous solution was added at the boiling stage with vigorous stirring. The solution was kept boiling for 15 min with stirring and additionally stirred for 15 min without heating. It has been known that citrate anions adsorbed on the Au particle surface act as a stabilizer. Colloidal Au particles were assembled on 3-aminopropyltriethoxysilane (APTES)-functionalized coverslip (Matsunami, borosilicate glass) and quartz (Shinetsu, Viosil) surfaces.[21] Briefly, glass substrates (18 × 18 × 0.5 mm) were cleaned by submerging in a 1:1 mixture of ammonia−water (28%) and aqueous hydrogen peroxide (30%) and dried. Then, the substrates were treated with a 2% methanol solution of APTES for 1 h at 60 °C. After silanization, surfaces were rinsed several times with methanol and then distilled water before being placed into solutions of Au NPs for 12−18 h at ambient temperature. The substrates assembled with Au NP films were rinsed with distilled water and dried.

Laser irradiation was carried out normal to the glass substrate by a single shot through a photomask with 3 mm diameter circular hole. Unfocused beam of a frequency-doubled output (532 nm) of a nanosecond Nd:YAG laser (Continuum Surelite I-10, pulse width: 6 ns; beam diameter: 6 mm) was employed. The glass substrates exposed to the laser shots were examined by the extinction spectroscopy (Hitachi, U-2010 spectrophotometer) and field emission scanning electron microscopy (FE-SEM, Hitachi S4700). For the observation of FE-SEM of the glass substrates, Pt−Pd alloy was sputter deposited. The sputtered particles were distinguished from Au particles because of their size of less than 5 nm diameter. The glass surface exposed to the laser irradiation was examined by SEM in the presence and absence of Au NPs. For removal of Au NPs, a part of an irradiated spot was scrubbed gently with a methanol-applied cotton paper (Asahi Kasei, BEMCOT). The cotton paper was tightly fixed around the pair of tweezers. As a compliment to a 2D measurement by SEM, topographical images were acquired by atomic force microscopy (AFM) on a Veeco Innova SPM with a probe tip of a radius of curvature of 2 nm (NANOWORLD SSS-NCH-10).

RESULTS

Exposure of a glass substrate assembled with Au NPs to a single-shot of a 532 nm nanosecond pulsed-laser light allowed for the observation of remarkable morphological alterations for both NPs and the glass surface depending on the applied laser fluence. Figure 1 depicts the SEM images of the irradiated surface at a fluence of 360 mJ cm^{-2} $pulse^{-1}$.

In Figure 1, the inset depicts intact Au particles. A large population of as-prepared particles assume an oblate shape with an average diameter (an average of long and short axes) of 47 ± 8 nm. The left side of the image represents the irradiated surface that is fully covered with Au NPs appreciably smaller in size than the original particles shown in the inset. The formation of the small particles is caused by pulsed laser-induced fragmentation, a phenomenon observed previously in solutions.[22−26] By contrast, the right side of the SEM image represents the bare glass surface that was exposed after the irradiation by removing Au particles such as those seen on the left side of the SEM image. The occurrence of small craters of approximately 10 nm diameter is remarked as scattered dark spots, each surrounded by bright circle. A strong support for the assignment to the craters is obtained by the observation of AFM images of the glass surfaces exposed to the laser irradiation, Figure 2.

Inspection of Figure 2 clearly revealed the presence of pitted spots (shown by dark spots) corresponding to the craters observed by SEM. The diameter of the craters observed by AFM is

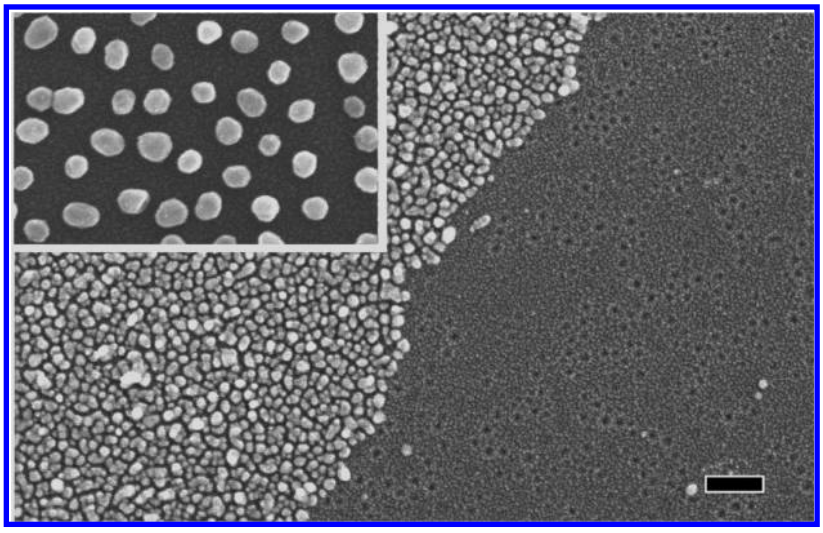

Figure 1. SEM image of a borosilicate glass surface assembled with 47 ± 8 nm Au NPs with a surface coverage of 30% and exposed to a single-shot of a 532 nm pulsed laser light (fluence: 360 mJ cm^{-2} $pulse^{-1}$). The left side of the image shows the glass surface fully covered with small NPs resulting from the laser-splitting of the original particles. The right side of the image displays a bare surface from which the particles were removed after the laser irradiation. Here, many dark spots with a slightly bright outer ring are formed on the bare surface. These spots correspond to craters formed by the laser irradiation as revealed by the AFM measurement (see Figure 2). For comparison, inset depicts the SEM image of the glass surface before the irradiation. The scale bar represents 100 nm.

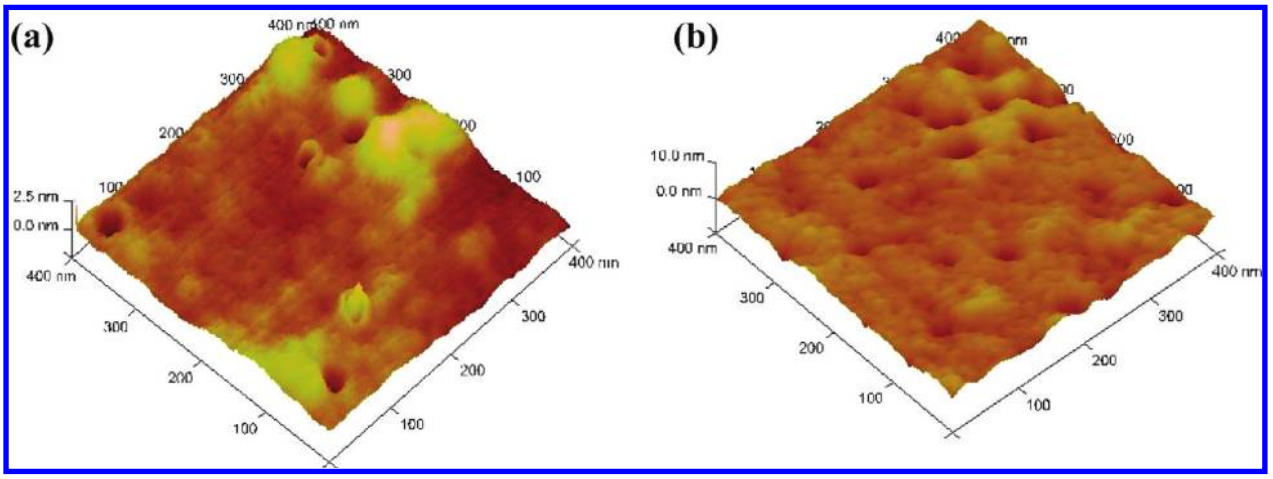

Figure 2. AFM topographical images of sample surfaces subjected to a single shot laser irradiation at laser fluences of 226 mJ cm^{-2} (a) and 470 mJ cm^{-2} (b). Dark spots represent pitted areas corresponding to the craters. The average crater depth is 2 nm in (a) and 4−6 nm in (b). The AFM images were acquired for the surfaces exposed to the laser irradiation and in the absence of Pt−Pd coating. The fragments of Au particles were removed before the measurement.

approximately 20 nm that was greater than that of ca. 10 nm observed by SEM. This discrepancy might be due to the fact that the 2D SEM image is not appropriate for estimating shallow crater diameters. Moreover, the depth of the craters measured by AFM is dependent on the laser fluence imparted: approximately 2 nm at 226 mJ cm^{-2} and 4−6 nm at 470 mJ cm^{-2}. Consistent with this observation, the SEM image of the craters at low fluences carries a low image contrast because of a shallow nature and the prolonged irradiation of the electron beam for the observation stimulated the flattening of the craters due to the melting of the glass surface. At high fluences, however, the SEM pictures gave a clear image contrast and the melting during the SEM observation is less pronounced. The SEM images showing the effect of laser fluences were given in Supporting Information, Figure S1. It is interesting to note that the repeated laser irradiations of 100−1000 shots permitted the enlargement of the structures to a hundred up to several hundred nanometer-sized craters.[19]

The number density of the craters formed by a single laser shot strongly depends on the laser fluence applied. The number density estimated from SEM images is depicted in Figure 3 as a function of laser fluence. The number density exhibits a sharp rise with increasing laser fluence and its onset was observed at 160−170 mJ cm^{-2} $pulse^{-1}$. Consistent with the SEM observation, a laser fluence-dependent increase of the population of the craters was also observed for the AFM images (Figure 2).

Most importantly, the crater formation on the glass surface is closely associated with the laser-induced transformation of Au NPs. We observed the morphological changes of the NPs upon irradiation at various laser fluences. Figure 4 shows the particle

size distribution extracted from SEM micrographs as a function of laser fluence. Figure 4a gives the size distribution for intact particles, and panels b−d show the results of laser irradiation. With increasing laser fluences, the splitting of NPs starts to take place with a threshold at 180 mJ cm^{-2} $pulse^{-1}$ (Figure 4b). Generally, a bimodal particle size distribution consisting of a size similar to the original particles and fragments was observed as a result of laser irradiation although the fragments carried a considerably broad size distribution. We note here that particles remaining without undergoing fragmentation are remarkably spherical (see the difference of SEM images between panels a and b in Figure 4) because of melting. The number of particles that fail to undergo splitting decreases with increasing laser fluences. At the fluence of 225 mJ cm^{-2} $pulse^{-1}$, approximately 40% of the original particles undergoes splitting (Figure 4c). Furthermore, at the fluence of 275 mJ cm^{-2} $pulse^{-1}$, the original particles were entirely fragmented (Figure 4d). Close examination of Figure 4 reveals that the laser-induced splitting is responsible for the crater formation because the onset of the slitting of Au NPs in terms of laser fluence (180 mJ·cm^{-2}·$pulse^{-1}$) coincides with the onset of crater formation (160−170 mJ cm^{-2} $pulse^{-1}$) and the increase in the number density of craters well correlates with the increase in the number density of particles undergoing splitting.

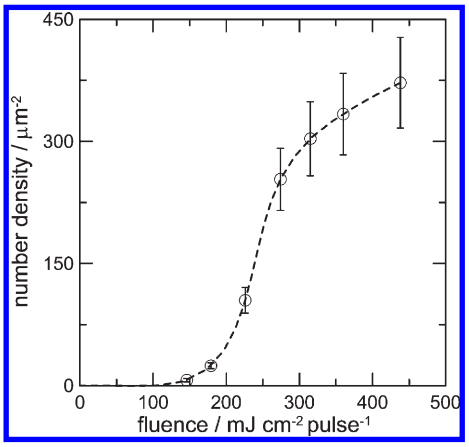

Figure 3. Number density of craters as a function of laser fluence for a single-shot laser irradiation. The number density of original Au NPs was 150 ± 10 particles μm^{-2}.

Finally, we measured the extinction spectral evolution (Figure 5) of the Au-modified glass substrate irradiated at various laser fluences in order to acquire information complementary to that obtained by SEM observation. It has been established that the extinction spectrum of Au NPs strongly reflects the particle size and shape, spacing, and the refractive index of surrounding medium.[1] Before the laser irradiation, the extinction spectrum was measured consisting of two peaks: one at 520 nm which is ascribed to the surface plasmon resonance band of pseudospherical Au

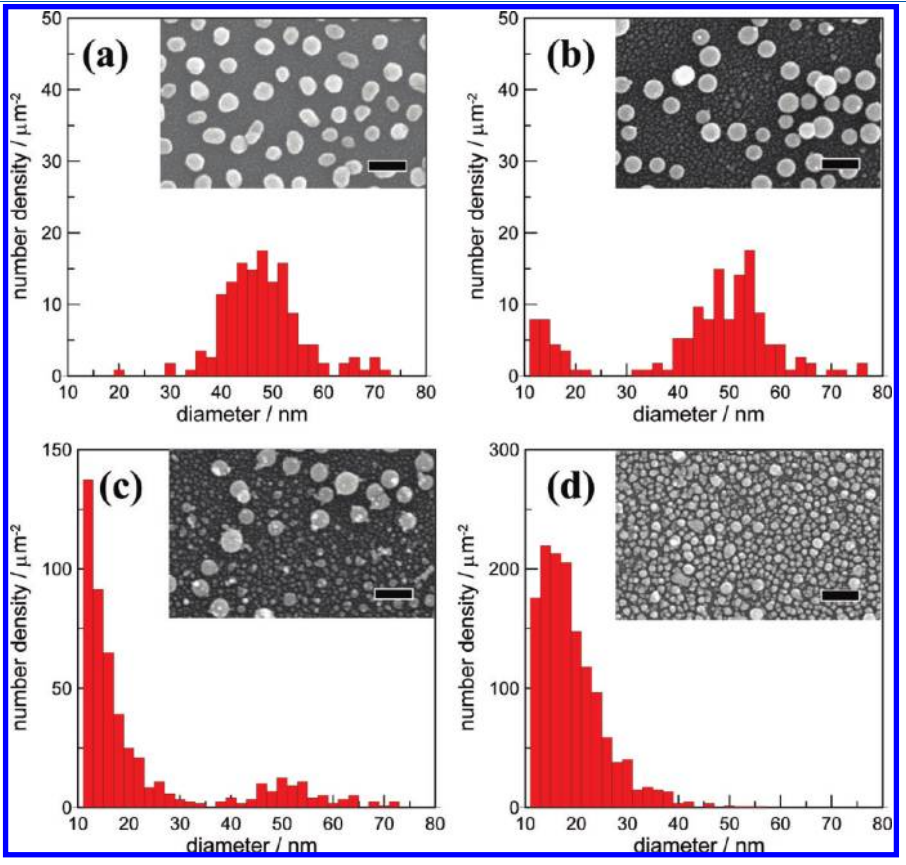

Figure 4. Particle size distribution on glass surface exposed to a single-shot laser light of various fluences from SEM image analyses. A part of original SEM image was given in the inset of each panel. Panels a−d represent the distribution for various laser fluences: (a) 0 mJ cm^{-2} $pulse^{-1}$ (before irradiation), (b) 180 mJ cm^{-2} $pulse^{-1}$, (c) 225 mJ cm^{-2} $pulse^{-1}$, and (d) 275 mJ cm^{-2} $pulse^{-1}$. The particle diameter of intact Au NPs is 47 ± 8 nm. Particles less than 10 nm diameter were not counted for constructing the histograms because of resemblance in size with sputter-deposited Pt−Pd particles with an average diameter of 5 nm for SEM observations. Note that the ordinate scale in panel a is the same as that in panel b but smaller than the scales in panels c and d because of increased number of particles due to efficient splitting at high laser fluences. The scale bars represent 100 nm.

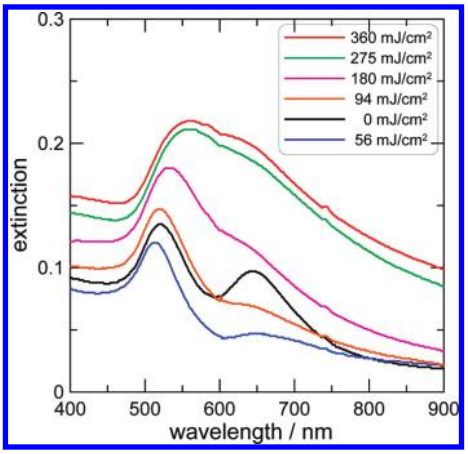

Figure 5. Extinction spectra of Au-NP modified (Au NP diameter: 47 ± 8 nm, coverage: 30%) glass substrate exposed to a single-shot laser light of various fluences given in the inset.

particles[1] and the second at 650 nm which presumably originates from dimer or associated particles.[27−29] The dimeric species and associated particles were observed in SEM pictures (see Figure 4 (a)). Laser irradiation altered remarkably the spectral shape. For instance, the contribution of the low energy peak is reduced regardless of the laser fluence, which is ascribed to the reduction in the population of the associated particles due to melting and splitting. Additionally, broad spectral envelopes with a peak shift to longer wavelengths were observed for samples irradiated at relatively high fluences. On increasing the laser fluence, steady increase was observed for the baseline of the entire spectrum. This is caused by the large-scale aggregation of small particles observed by the SEM images as reported previously.[30] The possibility that the increased baseline is resulting from the increased extinction of the substrate itself because of the nanocrater formation is denied. This is because the baseline was unchanged by one laser shot regardless of the fluence when the spectrum of irradiated substrate was measured after removal of the particles.

DISCUSSION

Our observation of nanosized craters on the visible laser irradiation of Au NP-assembled glass substrates is distinct from the previous observations of laser-induced nanofabrication. For instance, nanoholes prepared previously by a single-shot femtosecond laser irradiation on Si substrates possessed a size similar to or larger than that of Au particles.[12−14] Presently, however, the size of craters on glass substrates by a single nanosecond pulsed-laser irradiation is much smaller than that of NPs because of the fragmentation (Figure 1). Besides this, the number density of craters increased with increasing laser fluences above the threshold and exceeded that of original Au particles at high fluences (Figure 3) while each Au NP produced one nanohole on Si. In reality, the resonant coupling of Au NPs with their mirror image in a glass substrate, i.e., the mirror image effect,[31] should be weaker than that for Si because of the lower permittivity, which causes lower enhancement of the electromagnetic field in the area around the contacting point on the substrate. Therefore, we can safely exclude the possibility that the craters are formed by the ablation of the glass surface resulting from a multiphoton absorption due to the enhanced electromagnetic field of light by the plasmon band excitation. Instead, a role played by the

Scheme 1. Pictorial Representation of the System

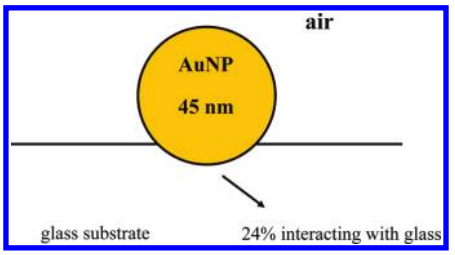

photothermal and photomechanical effects by the excitation of the plasmon band of Au NPs should be taken into consideration because the crater formation takes place simultaneously with the splitting of Au NPs placed on the substrate (Figure 4).

The problem of Au NP heating and heat transfer to the surrounding environment under a variety of laser exposure conditions and particle properties have been studied previously.[32−34] We employed a couple of heat equation as given in eq 1 for estimating the lattice temperature of Au NP, T_l and the temperature of the surrounding medium, T_m, resulting from the heat transfer.

$$C_l(T_l)\frac{dT_l(t)}{dt} = -F + S(t) \tag{1a}$$

$$C_m\frac{\partial T_m(r,t)}{\partial t} = k_m\frac{1}{r^2}\frac{\partial}{\partial r}\left(r^2\frac{\partial T_m(r,t)}{\partial r}\right) + F \tag{1b}$$

Here C represents the heat capacity (C_l for Au and C_m for the surrounding medium), F is the heat dissipation term, S is the input energy of laser, and k_m is the thermal conductivity of the surrounding medium associated with heat diffusion. The first term on the right side in eq 1b represents the heat diffusion with r, distance to the particle center. The laser energy term, S [W m^{-3}], absorbed by the unit volume, V_p [m^3], of a spherical particle of radius R [m] with a Mie absorption cross section of C_{abs} [m^2] in the medium with a refractive index of n_m is defined by eq 2

$$S(t) = \frac{C^{\lambda}_{abs}(n_m,R)\,P(t)}{V_p(T_l)} \tag{2}$$

In eq 2, P [W m^{-2}] is the laser power dependent on time, t, at the maximum of the spatial Gaussian profile. The volume, V_p, is dependent on the lattice temperature, T_l, because of the volume expansion in both solid and liquid phases, and C_{abs} depends largely on the refractive index of surrounding medium, n_m, as well as exciting laser wavelength and the size of NP. The heat dissipation term F was derived empirically by Plech and coworkers as eq 3[35]

$$F = \frac{3h}{R(T_l)}[T_l - T_m(R)] \tag{3}$$

where h denotes the interface thermal conductance and $R(T_l)$ is temperature dependent radius of Au NP. Now the question is how we can define the medium for the present system of Au NPs surrounded by air and placed on a glass surface.

The extinction spectrum of intact particles given in Figure 5 provides information on n_m by the calculation of an extinction cross section, C_{ext} at 532 nm of 2.12 × 10^{-15} m^2 for a 45 nm Au NP from the particle number density of 150 μm^{-2} and extinction

dx.doi.org/10.1021/jp106830x |J. Phys. Chem. C 2011, 115, 4986–4993

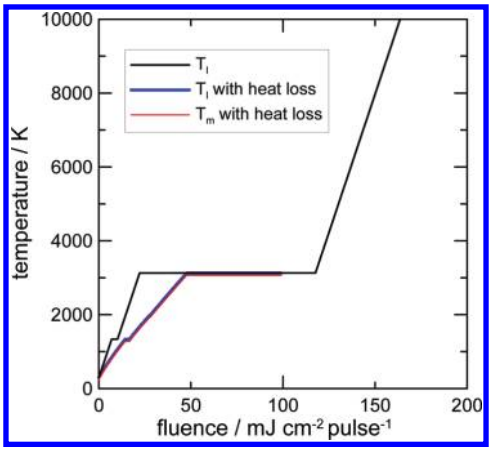

Figure 6. Rise in temperatures, T_l and T_m, as a function of laser fluence for a 45 nm diameter Au nanoparticles exposed to a pulsed laser light (532 nm, 5 ns) estimated by calculation both in the absence and in the presence of heat dissipation.

at 532 nm of 0.138, by applying the Mie theory.[36] Linear interpolation of the derived C_{ext} allowed the estimation of n_m = 1.12 for the present medium located between n_m = 1.00 in air (C_{ext}(532 nm) = 1.11 × 10^{-15} m^2 for 45 nm Au) and n_m = 1.50 in glass (C_{ext}(532 nm) = 6.125 × 10^{-15} m^2 for 45 nm Au). We estimated that a quarter of the surface area of the NP interacts with the glass surface to undergo heat transfer (Scheme 1) through the linear interpolation of the value of n_m (n_m = 1.12) between 0% (n_m = 1.00) and 100% glass medium (n_m = 1.50). Thus the heat dissipation term in eq 3 is corrected for the contribution of the NP surface area interacting with the glass surface relative to the total surface area of the NP as F' given by

$$F' = \frac{3h}{4R(T_l)}\left[T_l - T_m(R)\right] \qquad (3')$$

The value of 190 × 10^6 W m^{-2} K^{-1} for h in eq 3′ is obtained from the literature for silver NP embedded in glass.[32] The heat equation in the absence of heat dissipation is obtained by setting F = 0 and k_m = 0 in eq 1a.

A numerical simulation based on eq 1−3′ allowed the estimation of T_l and T_m at various delay times and laser fluences. Figure 6 shows the temperature curves as a function of laser fluence both in the absence and in the presence of heat dissipation to the glass substrate after 5 ns of the laser excitation. Additionally, examples of the time-dependent evolution of the temperatures were given in Supporting Information, Figure S2 to show how fast the heat transfer takes place. Inspection of Figure 6 reveals that fair degree of heat transfer to the substrate takes place but not affecting significantly the rise of T_l because of the fast supply of sufficient heat energy during the laser pulse, causing only a shift of the temperature curve of T_l to a larger fluence than that in the absence of heat dissipation. Note that our calculation of heat dissipation is up to the boiling point of Au because it is difficult to deal with the event of evaporation of Au, simultaneously with the heat dissipation.

The laser energy that can raise the temperature of a whole particle above the boiling point of 3243 K for 45 nm diameter Au particle is 120 mJ cm^{-2} $pulse^{-1}$ in the absence of heat dissipation and approximately 150 mJ cm^{-2} $pulse^{-1}$ in the presence of heat dissipation to the medium. The latter value is close to the onset of laser energy that initiates the crater formation (180 mJ cm^{-2} $pulse^{-1}$) and that of laser fragmentation of Au particles (160−170 mJ cm^{-2} $pulse^{-1}$). This strongly suggests that the boiling of the entire particle can channel into the explosive splitting of Au NPs,[37] resulting in potential damages to the surface through the collision of fragments with high kinetic energy. In other words, the fragments of Au NPs can drill the glass surface. Ito and coworkers demonstrated the laser ablation of a single Au NP with a diameter of 80 nm on a glass substrate submerged in water by a single-shot irradiation of 355 nm nanosecond pulsed-laser.[38] They observed that the Au NPs are fragmented on the surface at the initial stage of laser ablation and the resultant fragments are adhered strongly to the glass surface. This adhesion means that the fragments were blown attached to the surface, indicative of remarkably large kinetic energy carried away by the fragments although they did not look into the glass surface.

The reason for the increase in the number of craters with increasing laser fluence can primarily be associated with increased number of original particles undergoing splitting at high fluences. Obviously, the light absorption cross section of NPs changes depending on the particle size, aggregation, and local environment as depicted in Figure 5. Therefore, large or aggregated particles, which exhibit relatively large absorption, may undergo splitting first at the onset of the laser ablation. The number of particles failed to undergo fragmentation remarkably decreased with increasing pulse energy, because of an increased laser fragmentation probability at high fluences. This reflects the fluence-dependent particle size distribution in which the number of small particles increases at the expense of large particles. Moreover, we observed that the number density of craters finally exceeds the original Au particles (Figure 3). This can be explained by the assumption that more than one fragments or clusters emitted from the original particles can contribute to the nanocrater formation while all the particles are undergoing splitting.

In order to check the validity of the drilling mechanism by the action of the fragments, we estimate a thermoacoustic pressure in the vicinity of the NP surface on instantaneous (nanosecond) laser heating. We calculated the vapor pressure, p_0, of solid gold at a given temperature, T (K) on the basis of Einstein model of the solid according to eq 5[39,40]

$$p_0 = \frac{(2\pi m)^{3/2}}{(k_B T)^{1/2}} \nu_0^3 \exp\left(\frac{-L_0}{k_B T}\right) \qquad (5)$$

where m represents atomic mass of gold; ν_0, lattice vibration frequency; L_0, sublimation energy; and k_B, Boltzmann constant. The values of ν_0 = 3.0 × 10^{12} s^{-1}, L_0 = 3.82 eV for gold can be found in the literature.[41] The temperatures of Au NP used in the calculation of p_0 are those in the absence of heat dissipation as given in Figure 6, because, in our model, the calculation of temperatures above the boiling point is not possible in the presence of heat dissipation. This may cause somewhat overestimation of temperatures in calculating p_0 using eq 5. The resultant pressure was given in Figure 7 as a function of laser fluence for a 45 nm diameter gold particle. We expect that, in the presence of heat transfer to the medium, the stress curve given in Figure 7 may undergo slight shift to the right side. The result indicates that the order of magnitude of the pressure generated by the evaporation of gold itself is very large, far exceeding a pressure wave and shock wave generated in the medium by the laser heating of Au NPs below the boiling temperature because the latter takes a range of values within the order of MPa.[42]

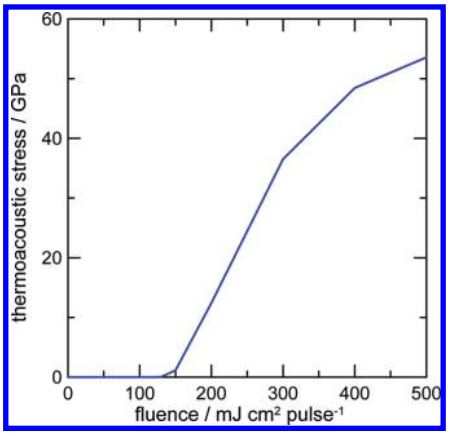

Figure 7. Thermoacoustic pressure estimated by the vapor pressure of gold given in eq 5 as a function of laser fluence for 45 nm diameter Au NPs placed on a glass substrate (effective refractive index: 1.12). The temperatures of the NP used in the calculation of p_0 are those in the absence of heat dissipation given in Figure 6.

Remarkably, a sharp rise was observed in the gold vapor pressure as a function of laser fluence with a onset of 120 mJ cm^{-2} pulse^{-1}.

The onset value of crater formation may depend on the durability of a host material. For instance, a measure of hardness, the Vicker's hardness of the borosilicate glass gives a value of 5−6 GPa,[43] which corresponds to the thermoacoustic pressure estimated for the onset of particle explosion. Generally, substrates may undergo damages if a generated pressure exceeds the tolerance limit of materials and then the actual onset of crater formation is determined. In order to confirm this assumption, we attempted the crater fabrication on a quartz substrate (see the Supporting Information, Figure S3). In this case, a greater value of the Vicker's hardness of 8.9 GPa[44] predicts a larger onset value of crater formation. Indeed, the crater formation threshold of >300 mJ cm^{-2} pulse^{-1} was observed despite that the exact value was difficult to determine by the SEM observation. Apparently, the quartz substrate has greater durability to the damage caused by this treatment than the borosilicate substrate. This is consistent with the assumption that the crater formation is initiated by a local high pressure and the hardness can determine the onset, even though another factor such as the modified absorbance of Au NPs due to the local refractive index change can be involved.

SUMMARY

The present work is regarded as the extension of a pulsed-laser induced ablation/fragmentation of Au NPs in liquids[22−26] to the solid surface where the substrate, instead of solvents, serves as a thermal energy acceptor. The extension allowed the observation of a single shot visible laser-induced photomodification represented by the nanocrater formation at unspecified places on the surface of the glass substrate. This observation is mechanistically different from the previous finding of nanoholes generated on silicon substrates due to the plasmonic enhancement of the electromagnetic field in the close vicinity of NPs,[12−14] because the laser-induced splitting of the NPs plays a crucial role. We obtained the result indicating that the laser-splitting of NPs is directly connected to the nanocrater formation through the process in which fragments carrying a large kinetic energy generated by the explosive evaporation of the Au NPs hit the glass surface causing damages. The calculation of thermoacoustic stress as a gold vapor pressure caused by sudden temperature increase by laser irradiation gave a solid support for the mechanism. Our present finding is important because additional laser irradiations allow the enlargement of the craters. Furthermore, the photomodified area after prolonged irradiation acquires increased susceptibility to the etching by hydrofluoric acid.[19] This may open up a possibility to the NP-assisted structuring of glass surfaces, which permits the local modification of wettability, transparency, roughness, and chemical structure with a considerably low intensity of laser light. Such effort in pursuit of the energy saving way of fabrication is now underway.

ASSOCIATED CONTENT

Supporting Information. Laser fluence-dependent modifications of a glass surface observed by SEM images, time-dependent evolution of lattice temperature of Au NP in the presence and absence of heat transfer to the surrounding medium, and SEM image of nanocraters formed on quartz substrate. This material is available free of charge via the Internet at http://pubs.acs.org.

AUTHOR INFORMATION

Corresponding Author
*E-mail: hashi@eco.tokushima-u.ac.jp.

ACKNOWLEDGMENT

Financial support by KAKENHI, no. 22655043 from JSPS and no. 21020025 on Priority Area "Strong Photon-Molecule Coupling Fields (No. 470)" from the MEXT of Japanese government, to S.H. is gratefully acknowledged. T.U. is grateful to the MOE-ATU Project (National Chiao Tung University) from the Ministry of Education of Taiwan and the National Science Council of Taiwan (NSC 98-2113-M-009-013-MY2). Mr. Tomoyuki Ueki is acknowledged for SEM photograph acquisition, and Mr. Yoshinori Nakagawa is acknowledged for the measurement of AFM. Special thanks are due to Mr. Daniel Werner who helped us to calculate heat dissipation.

REFERENCES

(1) Kreibig, U.; Vollmer, M. *Optical Properties of Metal Clusters*; Springer: Berlin, 1995.
(2) Weitz, D. A.; Garoff, S.; Gersten, J. I.; Nitzan, A. *J. Chem. Phys.* **1983**, *78*, 5324–5338.
(3) Kneipp, K.; Kneipp, H.; Itzkan, I.; Dasari, R. R.; Feld, M. S. *Chem. Rev.* **1999**, *99*, 2957–2975.
(4) Pieczonka, N P. W.; Aroca, R. F. *Chem. Soc. Rev.* **2008**, *37*, 946–954.
(5) Nishi, H.; Asahi, T.; Kobatake, S. *J. Phys. Chem. C* **2009**, *113*, 17359–17366.
(6) Tsuboi, Y.; Shimizu, R.; Shoji, T.; Kitamura, N. *J. Am. Chem. Soc.* **2009**, *131*, 12623–12627.
(7) Link, S.; El-Sayed, M. A. *Annu. Rev. Phys. Chem.* **2003**, *54*, 331–366.
(8) Hartland, G. V. *Annu. Rev. Phys. Chem.* **2006**, *57*, 403–430.
(9) Pustovalov, V. K.; Smetannikov, A. S.; Zharov, V. P. *Laser Phys. Lett.* **2008**, *11*, 775–792.
(10) Ko, S. H.; Choi, Y.; Hwang, D. J.; Grigoropoulos, C. P. *Appl. Phys. Lett.* **2006**, *89*, 141126.
(11) Yamada, K.; Itoh, T.; Tsuboi, Y. *Appl. Phys. Express* **2008**, *1*, No. 087001.
(12) Nedyalkov, N. N.; Takada, H.; Obara, M. *Appl. Phys. A: Mater. Sci. Process.* **2006**, *85*, 163–168.

(13) Nedyalkov, N. N.; Sakai, T.; Mianishi, T.; Obara, M. *J. Phys. D: Appl. Phys.* **2006**, *39*, 5037–5042.
(14) Nedyalkov, N. N.; Atanasov, P. A.; Obara, M. *Nanotechnology* **2007**, *18*, 305703.
(15) Leiderer, P.; Bartels, C.; Konig-Birk, J.; Mosbacher, M.; Boneberg, J. *Appl. Phys. Lett.* **2004**, *85*, 5370–5372.
(16) Heltzel, A.; Theppakuttai, S.; Chen, S. C.; Howell, J. R. *Nanotechnology* **2008**, *19*, No. 025305.
(17) Gattass, R. R.; Mazur, E. *Nat. Photonics* **2008**, *2*, 219–225.
(18) Juodkazis, S.; Mizeikis, V.; Matsuo, S.; Ueno, K.; Misawa, H. *Bull. Chem. Soc. Jpn.* **2008**, *81*, 411–448.
(19) Hashimoto, S.; Uwada, T.; Hagiri, M.; Takai, H.; Ueki, T. *J. Phys. Chem. C* **2009**, *113*, 20640–20647.
(20) Frens, G. *Nature Phys. Sci* **1973**, *241*, 20–22.
(21) Keating, C. D.; Musick, M. D.; Keefe, M. H.; Natan, M. J. *J. Chem. Educ.* **1999**, *76*, 949–955.
(22) Takami, A.; Kurita, H.; Koda, S. *J. Phys. Chem. B* **1999**, *103*, 1226–1232.
(23) Yamada, K.; Miyajima, K.; Mafune, F. *J. Phys. Chem. C* **2007**, *111*, 11246.
(24) Shoji, M.; Miyajima, K.; Mafune, F. *J. Phys. Chem. C* **2008**, *112*, 1929.
(25) Werner, D.; Hashimoto, S.; Uwada, T. *Langmuir* **2010**, *26*, 9956–9963.
(26) Amendola, V.; Meneghetti, M. *J. Mater. Chem.* **2007**, *17*, 4705–4710.
(27) Su, K.-H.; Wei, Q.-H.; Zhang, X.; Mock, J. J.; Smith, D. R.; Schultz, S. *Nano Lett.* **2003**, *3*, 1087–1090.
(28) Jain, P. K.; Huang, W; El-Sayed, M. A. *Nano Lett.* **2007**, *7*, 2080–2088.
(29) Lazarides, A. A.; Schatz, G. C. *J. Phys. Chem. B* **2000**, *104*, 460–467.
(30) Shibamoto, K.; Sakata, K.; Nagoshi, k.; Korenaga, T. *J. Phys. Chem. C* **2009**, *113*, 17774–17779.
(31) Feidj, N.; Aubard, J.; Lei, G.; Krenn, J. R.; Salerno, M.; Schider, G.; Lamprecht, B.; Leitner, A.; Aussenegg, F. R. *Phys. Rev. B* **2002**, *65*, No. 075419.
(32) Kotaidis, V.; Dahmen, C.; Von Plessen, G.; Springer, F.; Plech, A. *J. Chem. Phys.* **2006**, *124*, 184702.
(33) Ekici, O.; Harrison, R. K.; Durr, N. J.; Eversole, D. S.; Lee, M.; Ben-Yakar, A. *J. Phys. D: Appl. Phys.* **2008**, *41*, 185501.
(34) Sassaroli, E.; Li, K. C. P.; O'Neil, B E. *Phys. Med. Biol.* **2009**, *54*, 5541–5560.
(35) Plech, A.; Kotaidis, V.; Grésillon, S.; Dahmen, C.; Von Plessen, G. *Phys. Rev. B* **2004**, *70*, 195423.
(36) Bohren, C. F.; Huffman, D. R. *Absorption and Scattering of Light by Small Particles*; Wiley: New York, 1983.
(37) The Coulomb explosion mechanism[23,24] is not applicable to the present case because of low laser fluences employed (< 0.5 J cm^{-2} pulse^{-1}). The Coulomb explosion mechanism is only feasible for irradiations by high power lasers such as femtosecond lasers and nanosecond lasers with extremely high laser fluences (5−25 J cm^{-2} pulse^{-1}). Under the present experimental condition, only photothermal mechanism[22,25] is applicable. For details, see for instance: (a) Pyatenko, A.; Yamaguchi, M.; Suzuki, M. *J. Phys. Chem. C* **2009**, *113*, 9078–9085. (b) Giammanco, F.; Giorgetti, E.; Marsili, P.; Giusti, A. *J. Phys. Chem. C* **2010**, *114*, 3354–3363.
(38) Ito, S.; Mizuno, T.; Yoshikawa, H.; Masuhara, H. *Jpn. J. Appl. Phys.* **2007**, *46*, L241.
(39) Mutaftschiev, B. *The Atomistic Nature of Crystal Growth*; Springer: Berlin, Germany, 2010; p 45.
(40) An equation similar to eq 1 but slightly different one was given in ref 9.
(41) Venables, J. A. *Introduction to Surface and Thin Film Processes*; Cambridge University Press: Cambridge, UK, 2000; pp 11−15.
(42) Faraggi, E.; Gerstman, B. S.; Sun, J. *J. Biomed. Opt.* **2005**, *10*, No. 064029.
(43) de Bonfils, J.; Peuget, S.; Panczer, G.; de Ligny, D.; Henry, S.; Noel, P. Y.; Chenet, A.; Champagnon, B. *J. Non-Cryst. Solids.* **2009**, *356*, 388–393.
(44) Beake, B. D.; Smith, J. F. *Philos. Mag. A* **2002**, *82*, 2179–2186.